NASA

SPACE VEHICLE
DESIGN CRITERIA
(GUIDANCE AND CONTROL)

NASA SP-8033

SPACECRAFT EARTH HORIZON SENSORS

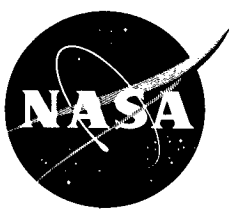

DECEMBER 1969

NATIONAL AERONAUTICS AND SPACE ADMINISTRATION

FOREWORD

NASA experience has indicated the need for uniform criteria for the design of space vehicles. Accordingly, criteria are being developed for the following areas of spacecraft technology:

Environment
Structures
Guidance and Control
Chemical Propulsion

Individual components of this work will be issued as separate monographs as soon as they are completed. This document, "Spacecraft Earth Horizon Sensors," is one such monograph. A list of all published monographs in this series can be found on the last page.

These monographs are to be regarded as guides to design and not NASA requirements, except as may be specified in formal project specifications. It is expected, however, that the criteria sections of these monographs, revised as experience may dictate, eventually will be uniformly applied in the design of NASA space vehicles.

This monograph was prepared under the sponsorship of the NASA Electronics Research Center by John R. Thomas and William L. Wolfe of the Honeywell Radiation Center with the assistance of Abe Manevitz, Alex Koso, and Bill McCracken of Honeywell and Prof. Stanley S. Ballard of the University of Florida. The effort was guided by an advisory panel chaired by Mr. Wolfe. The following individuals participated in advisory panel activities:

R. H. Anderson	Lockheed Missiles & Space Co.
R. W. Astheimer	Barnes Engineering Co.
J. Bebris	NASA, Electronics Research Center
R. F. Bohling	NASA, Office of Advanced Research and Technology
F. J. Carroll	NASA, Electronics Research Center
J. A. Dodgen	NASA, Langley Research Center
M. D. Earle	Aerospace Corp.
J. L. Hieatt	TRW, Inc.
S. A. Knight	Quantic Industries Inc.
W. J. Raskin	NASA, Goddard Space Flight Center
R. M. Reid	Lockheed Missiles & Space Co.
J. R. Thomas	Honeywell Radiation Center

CONTENTS

SPACECRAFT EARTH HORIZON SENSORS

1. INTRODUCTION

Earth horizon sensors have been used on most orbiting spacecraft because they provide a convenient means for indicating the local vertical. In many applications they are used as the sensory components of active attitude-control systems; in others, sensed data is used to correlate the orientation of instruments, antennas, etc., with the local vertical.

Early sensors fell short of performance goals because of various problems that resulted from a lack of knowledge of the radiation emitted by the Earth and because of radiation from interfering astronomical bodies, principally the Moon and the Sun. Many of these problems have not been completely solved within the horizon-sensor system; however, operational techniques have been evolved to forestall the effects of these problems from adversely affecting spacecraft systems that use the horizon-sensor-derived information.

Considerable effort has been directed to the determination of the best spectral region for defining the space-to-Earth discontinuity and providing the greatest immunity to unwanted radiation. Most frequently, sensors use the Earth's radiation in the infrared spectrum (from 2 to 30 micro meters (μm)).

Because sufficient operational data regarding ultraviolet, visible, and microwave sensors are not available, this monograph is devoted exclusively to the discussion of infrared Earth horizon sensors.

2. STATE OF THE ART

2.1 Historical Background

Horizon-sensor development began in 1958 on sensors used for Jupiter rocket reentry experiments and for the Air Force Discoverer program. The Jupiter sensor evolved into sensors used on the Mercury, Nimbus, Biosatellite, ESRO, Vela, and Agena programs. The Discoverer sensor evolved into sensors used on the OGO and Gemini programs.

The types of sensors that were developed during this period can be divided into three basic classes: scanners, edge trackers, and radiance balancers. (Each of these is described in subsequent paragraphs.) References 1 to 3 contain comprehensive discussions of the horizon-sensing problem, flight descriptions, and descriptions of numerous horizon sensors.

The detectors used in these sensors are longwave thermal detectors operating at room temperature, such as thermistors, metal bolometers, or thermopiles. Other detector materials, such as (Hg,Cd)Te and InSb may be used in future systems. However, at this time they are used only in laboratory equipment.

2.2 Scanners

Scanners are sensors that either mechanically, electronically, or passively (on a rotating vehicle) scan a large volume of object space with a scan pattern fixed relative to the sensor or vehicle. An example of a horizon sensor with a mechanical scanner is the conical scanner

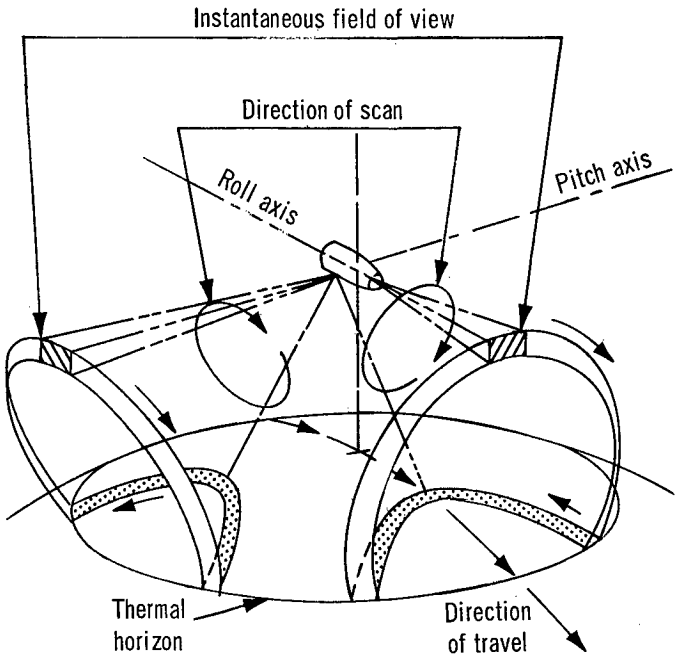

Figure 1.—Conical scan patterns.

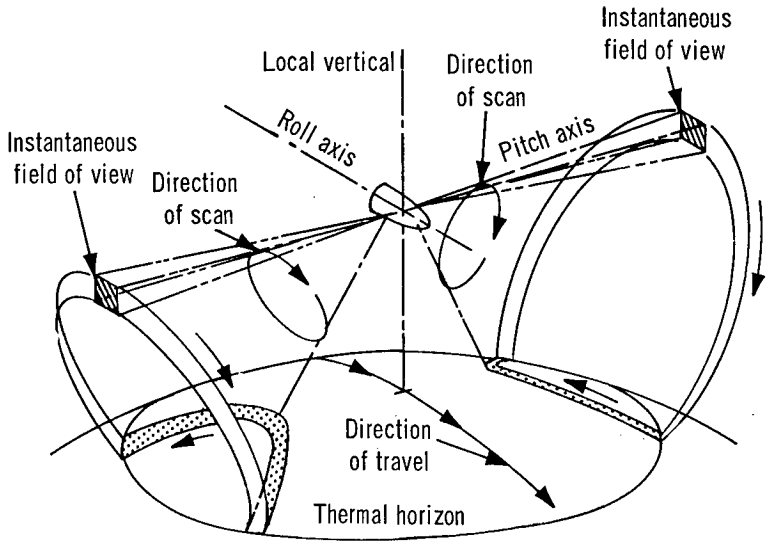

Figure 2.–Conical scan paths.

employed initially on Mercury vehicles. The evolution of this sensor is described in reference 4. In this type of scanner, two sensor heads are mounted on the satellite with their axes parallel to a pair of vehicle rotation axes. Refractive or reflective prisms or off-axis optics cause the field of view to be offset from the vehicle axis. When the optical element causing the offset is rotated by a motor, the field of view sweeps out a cone, which is centered about the vehicle axis. The two sensor heads can be mounted to the vehicle as indicated in figures 1 and 2.

The sensor determining pitch error is mounted so that the scan axis lies in the plane containing the vehicle pitch and yaw axes. The sensor generates a reference pulse when the field of view crosses this plane. The detector output signal in an ideal situation would be a square wave with amplitude proportional to Earth radiance and with width proportional to Earth-crossing time, or dwell time. If the Earth signal is centered about the reference pulse, the vehicle roll axis must be normal to the local vertical; this is the condition for zero pitch angle. Pitch attitude is proportional to the phase of the Earth pulse relative to the reference. Signal processing by a phase detector produces a dc signal proportional to the difference in phase between the Earth waveform and the reference pulse. Roll attitude can be obtained in a similar manner from another sensor mounted 90° away in yaw, as shown in figure 1, or from the difference in dwell times of two sensor heads in the configuration of figure 2.

The waveform obtained from scanning the Earth horizon is, however, not a pure square wave of constant amplitude. It is more nearly a ragged trapezoidal waveform with leading and trailing edges shifted in time relative to the horizon signal. These discrepancies are

caused by the detector time constant, the finite horizon crossing time, and nonuniformities in the horizon radiation. Electronic high-frequency boost is incorporated to compensate for these discrepancies, but at the cost of increased noise bandwidth. Because the signal amplitude is not constant during the Earth scan, the signal is limited by establishing a threshold on the amplified detector output as indicated in figure 3 (from ref. 2). Phase detection is not done on the actual detector signal but rather on the shaped output of the threshold sensing circuit. The shaped output is a constant amplitude square wave, the width of which, in the absence of clouds, is proportional to the width of the amplified detector signal at the threshold.

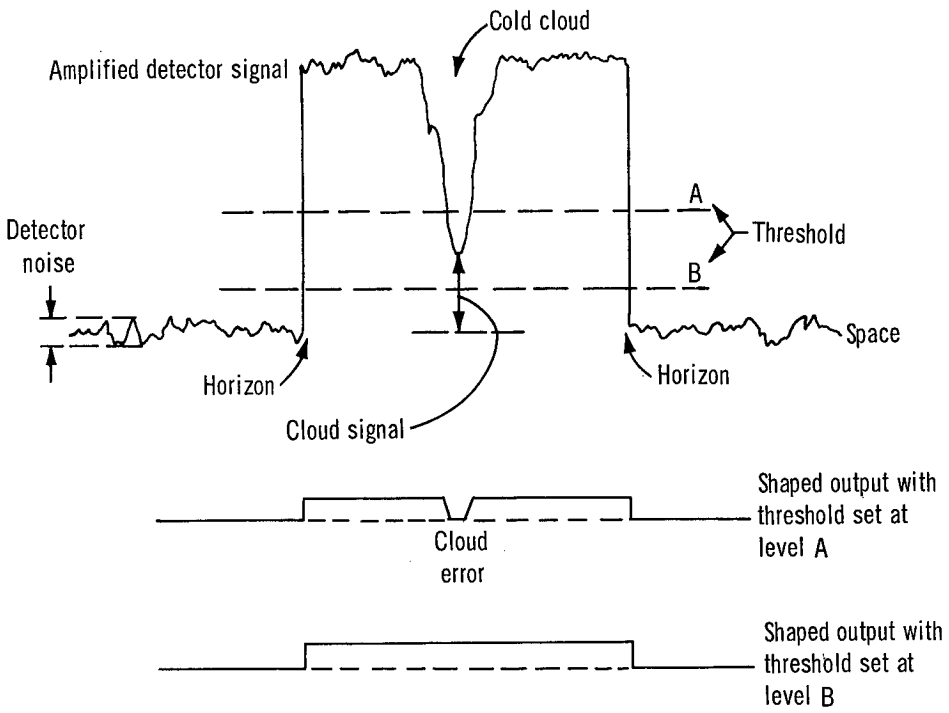

Figure 3.–Output waveshape for conical scan.

The nature of the cold-cloud problem faced by designers of early horizon sensors is also illustrated in figure 3. Because little data were available on the appearance of the Earth from space in the infrared region, estimates of the variation in detector signal across an Earth scan were, at best, coarse approximations. Furthermore, in an effort to minimize size and weight, the designers used the smallest possible aperture and the widest possible spectral region that bracketed the Earth's expected radiation (consistent with available materials).

22.1 Mercury Sensor

The Mercury horizon sensors utilized germanium optics with a spectral transmission extending from 1.8 to beyond 20 μm. This spectral region embraces the Earth's atmospheric window from about 8 to 14 μm and also the major absorption bands of the atmospheric constituents. Consequently, the sensor received radiation from both the atmosphere and the Earth's surface, the major portion from the latter. However, clouds are opaque in the 8-to-14-μm region and exist at high altitudes at temperatures considerably below that of the surface. When the detector field of view scanned across a cold cloud, the detector output signal dropped drastically, as illustrated in figure 3. When the signal dropped below the threshold level, a dropout in the shaped signal fed to the phase detector occurred, producing an error in the dc output of magnitude proportional to the size of the cloud.

The Mercury scanners employed a threshold level that was a fixed percentage of the peak signal, worsening the cloud problem. When the field of view crossed a hot horizon, the effective absolute threshold was raised (represented as level A). As can be seen in figure 3, this produced a greater cloud error. In some instances, when a cloud and a cold horizon followed a hot horizon, the edge of the cloud was sensed as the horizon, and large errors resulted. Output errors up to 35° were experienced (ref. 5). The errors were subsequently reduced when the threshold level was lowered to a minimum consistent with detector and electronic noise.

The Sun was the cause of three other problems for these Mercury sensors (ref. 5). First, Earth-reflected sunlight was greater than expected at the shorter wavelengths and produced Earth radiance nonuniformities. Second, when the Sun was near or directly in the scan path, the intensity of the Sun signal saturated the detector and electronics, requiring a recovery interval. Figure 4 (from ref. 3) is an MA-5 recording of amplified detector signals showing the relative Earth and Sun signals at times when the Sun was near the scan plane. Note that the Sun appears as a spike on one side of the scan and as an extended source on the other. Its largest subtense is about 80° of rotational scan angle. The third Sun-caused problem occurred during sunset when atmospheric filtering reduced the Sun signal below the Sun threshold level. The sensor could no longer discriminate between Earth and Sun, confusing the edge of the Sun with the Earth horizon. The sensed horizon at such times was displaced by 3° to 6°.

The Mercury sensor was also quite susceptible to EMI (electromagnetic interference) because of the low level of the detector signal—50 to 100 μV. Modifications were made to the spacecraft wiring and not to the sensor to alleviate the problem. The noise pickup problems were caused by inadvertently mounting the sensor heads in the ground plane of the spacecraft antennas.

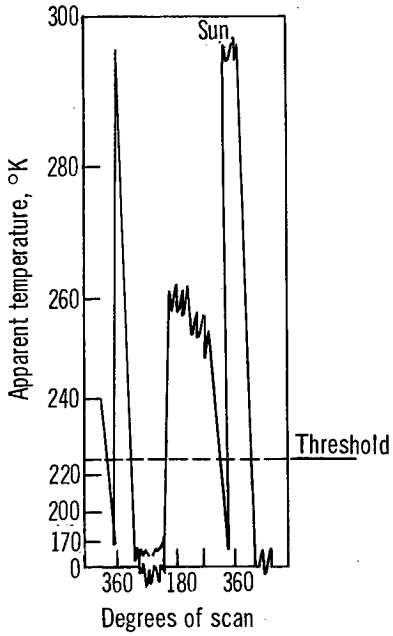

Figure 4.–Horizon sensor signal from Mercury scanner.

The problems enumerated thus far are typical of most horizon sensors. Their possibilities of occurrence were recognized before the first-generation sensor flights, but only flight experience uncovered their magnitude. The problem areas still exist, but their effects have been reduced. Conical scanner development has led to the following improvements:

(1) The spectral region of operation has been shifted to wavelengths beyond 14 μm, thus eliminating the atmospheric window responsible for most of the cloud effects. Operation at the longer wavelengths also reduced the solar signal by a factor of 100.
(2) The aperture has been increased and the number of refractive (and thus absorbing) elements has been reduced, thus increasing the detector signal.
(3) The detector field of view has been reduced in the scan direction and the scan rate has been reduced. Both of these changes increase the accuracy of the sensor because a smaller field of view gives a steeper horizon-crossing signal and a slower scan rate avoids time-constant problems in the electronics.
(4) Hyperimmersed detectors (ref. 6) have replaced immersed detectors to provide an increase in sensor optical gain.
(5) Electronic improvements have made possible preamplifier designs that reduce system noise.

(6) Low-speed hollow-shaft motors have replaced the high-speed motor/gear reduction drives of earlier sensors, thus increasing reliability.
(7) EMI filtering has been incorporated in the sensor.
(8) High-reliability electronic components have replaced commercial components (where required).
(9) Sun sensing by separate detectors and error compensations to reduce Sun error have been incorporated into some models. Sun on the horizon can still produce an error.

These improvements have not been achieved without a weight sacrifice. The Mercury horizon-sensor system weighed 8 lb. Present-day complete systems weigh approximately 25 lb.

Two of the most significant mechanical design improvements have been the elimination of gears and the addition of wick lubrication and labyrinth shields to extend sensor life in the event of loss of pressure (ref. 7). The lubricant evaporates from wick reservoirs and then condenses on the bearing and raceway surfaces. Labyrinth shields restrict the evaporation rate, provide lubrication for mission life, and prevent oil film coating of the optics.

2.2.2 Vela Satellite Sensor

Another type of scanning horizon sensor eliminates all friction-producing components by utilizing a scanning mirror mounted on flex pivots driven by a bearingless, brushless dc torque motor. This type of sensor is used on the Vela satellite, which operates at high orbital altitudes where the Earth subtends a much smaller angle. Consequently, the scan need not cover the angular range required by the Mercury-type orbits. The field of view sweeps back and forth across the Earth with a pulse generated at scan center. The scan center is alined to a vehicle reference. Each horizon crossing is threshold detected with the threshold set at a fixed percentage of the peak signal from that horizon. The scan angles between the reference pulse and the two horizon crossings then give attitude. The sensor launched on the Vela satellite in April 1967 has operated satisfactorily as of this writing. The spectral region used extends from 13.5 to 22 μm. Cloud sensitivity has not been a problem because of the spectral region used and because of the high-altitude orbit.

A Sun problem was found with this sensor. Even in the longer wavelength region used, the solar signal is still hundreds of times greater than the Earth signal. When the Sun was near the scan path and the horizon, the enormous Sun signal caused heating of the detector base, scattering, flare, and glare. The resultant detector output was below the established Sun threshold and comparable with Earth signal (ref. 7). The solar signal produced an effective solar diameter of up to 6°. Flight experience has shown that this signal could be interpreted falsely as the horizon and produce significant errors. However, because the satellite spins

about an axis alined to local vertical, Sun interference produces errors over a small part of a single vehicle rotation.

The problem was solved in the operation of the sensor by determining separately the impending solar interference and inhibiting the sensor output during the appropriate part of the vehicle rotation. The control system sampled the sensor output during that part of a rotation when the Sun was not in a position to cause interference.

The highly sensitive system also produced output signals caused by internally reflected infrared radiation. The solution to this problem was a redesigned lens barrel with better reflection attenuation.

2.2.3 Horizon-Crossing Indicator

A third type of wide-angle scanner is the passively scanned type used on Tiros and other spin-stabilized vehicles and referred to as a horizon-crossing indicator (HCI). It consists of a thermistor bolometer telescope mounted to a spinning vehicle, with the vehicle spin providing the scan. With the field of view direction offset an angle γ from the spacecraft spin axis, the output of the electronics would be similar to the preamplifier output of a conical scanner with a scan cone half-angle of γ. Horizon-crossing indicators are mechanically simple, but the other problems associated with HCI's are similar to those of the conical scanner and need not be discussed here. Further information is given in references 8 and 9.

2.2.4 Electronically Scanned Sensor

A fourth type of wide-angle scanner employs electronic scan of a detector array (ref. 10). An array of detectors, usually thermopiles, is arranged to have the desired total coverage in object space. The array is periodically sampled to determine which detectors are viewing Earth and which are viewing space, and attitude information is derived from this sampling using appropriate logic circuits. The problems with this scanner are closely related to the problems associated with radiance-balancing sensors, which are discussed in section 2.4.

2.3 Edge-Tracking Sensors

Edge tracking is achieved by driving a detector field of view to a particular location relative to the horizon. The field of view is dithered across the horizon by a servomechanism that

derives its error signal from the detector waveform. Alternatively, a static detector field of view could be servo-positioned to produce a preset dc output voltage. The former case will be discussed because there is more available flight experience for it; the latter sensing mechanism is more closely related to radiance balancing.

The two classic examples of the dithering field-of-view edge trackers are the OGO and Gemini trackers described respectively in references 11 and 12. OGO employs a horizon point-tracking scheme for tracking the horizon at four points around the horizon circle as illustrated in figure 5 (from ref. 11). Attitude information is derived from the simple geometric relationships between the four lines of sight to the horizon. Note that only three sight lines are required. The OGO sensor produces four sight lines in only two sensor heads; three lines are used in primary operation and the fourth is redundant. In the initial signal-processing design, a threshold on a fixed percentage of the peak detector output signal was used to generate a rectangular waveform. The oscillating field of view was controlled so that the average value of this waveform was zero. Thus the dither was centered on the threshold point.

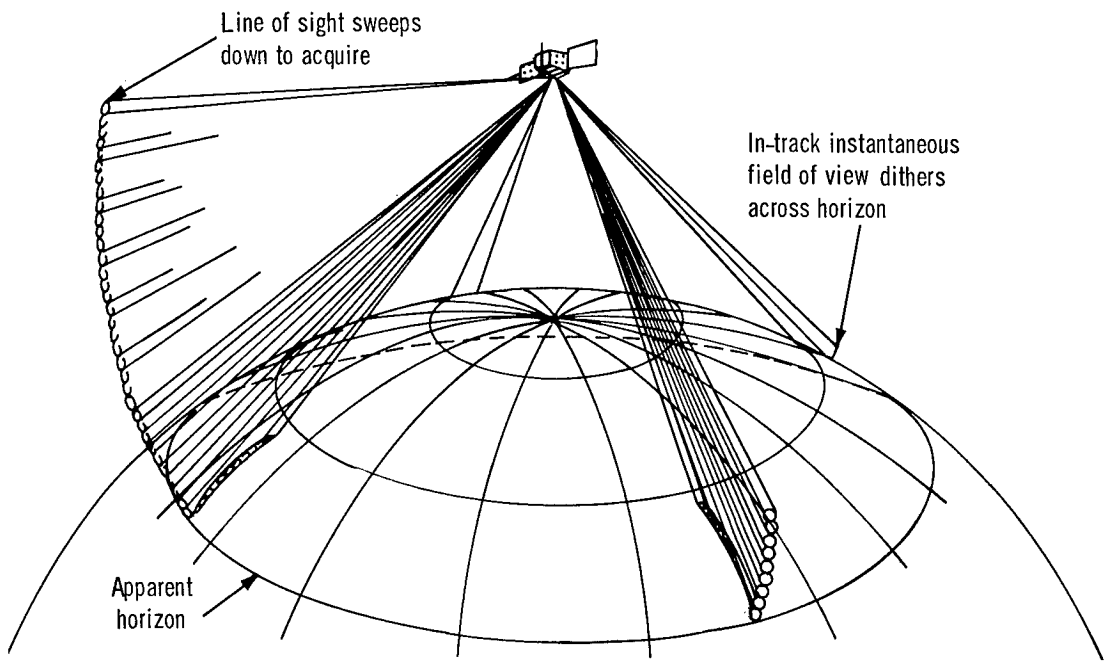

Figure 5.–Horizon point-tracking geometry.

The Gemini horizon sensor uses azimuth-scan edge tracking with a single field of view to track the horizon while the scanning head oscillates over about 160° in azimuth as shown in

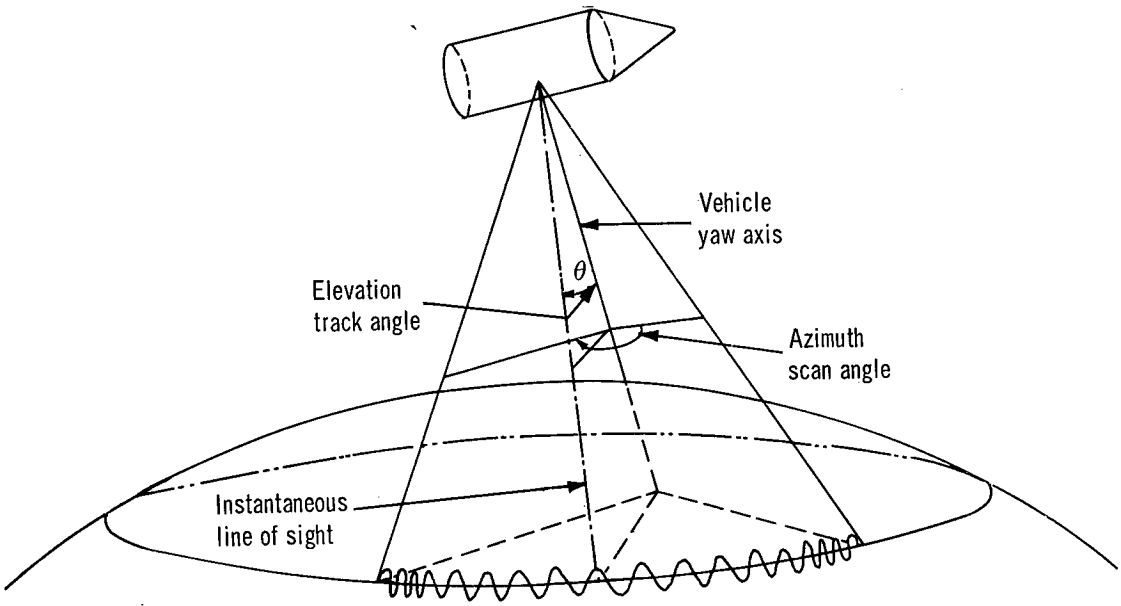

Figure 6.–Azimuth-scanning geometry.

figure 6 (from ref. 12). Tracking is achieved by synchronously demodulating the detector waveform at the dither frequency and driving the tracking mirror to produce a zero dc value of the demodulated signal. Only those quarter cycles of the detector waveform containing the horizon-crossing rise and fall times are demodulated; signals during the scan dwell time inside the horizon are gated out. Synchronous demodulation permits a much narrower electronic bandwidth than thresholding, with attendant lower noise voltage. References 1 and 12 contain derivations of the equations for the attitude signals, which are complicated functions of the time-varying azimuth and elevation angles of the field of view. The design evolution, including flight experience, is excellently documented in reference 13 for OGO, and reference 5 for Gemini; only the highlights are given here.

2.3.1 OGO Sensor

The most difficult problems in the development of the OGO horizon sensor were encountered in the design of the scan-mechanism flex pivots to withstand the vibration environment. Eventually, the unit performed flawlessly.

During thermal vacuum testing at both high temperature (120° F, 322° K) and low temperature (0° F, 255° K) and without external stimulus, signal amplifier noise increased to a level that kept the tracking logic in the track state. A low-pass filter was added to the signal amplifier output to correct the problem.

Radiated EMI grossly degraded sensor operation during the first system integration test when the 10-W transmitter in the spacecraft was turned on. Wiring changes in the sensor subassembly were made for better isolation from the transmitter.

A problem not documented in reference 13 occurred because of internally reflected and emitted infrared energy. Each sensor head was originally designed with a protective germanium window. The window produced multiple internal reflections of internal heat sources that were seen by the detector at the scan frequency. As a result, the sensor tracked itself. This problem was solved by removing the protective window and leaving the scan mechanism exposed to the space vacuum.

Test problems arose because of the nature of the sensor. The sensor was such a sensitive instrument that gradients in the test area other than the simulated horizon were tracked; even the corners of the room were tracked, and this made adequate testing of acquisition maneuvers impossible. Parallax between sensor heads viewing the relatively close simulated horizon introduced intolerable measurement errors. One sensor tracked a solar simulator. These latter two difficulties were overcome by source collimation and baffling, respectively.

On the first OGO flight, the sensor operated normally, but an experiment boom failed to deploy and blocked the sensor field of view so that operational data could not be obtained. The sensors were relocated on subsequent vehicles to prevent a recurrence.

On the second flight the sensors performed as designed. However, they tracked the edges of clouds that drifted into the sensor field of view during the orbital passage, as shown in figure 7 (from ref. 14). This caused the attitude-control system to orient the vehicle relative to the drifting cloud edges and resulted in depletion of the reaction jet fuel in 10 days instead of the intended 1 yr. The initially chosen spectral region (8 to 20 μm) permitted the sensor to "see" clouds. This problem was not discovered prior to flight because of insufficient dynamic simulation of clouds drifting through the field of view. The spectral region was changed subsequently by blocking below 13 μm, blinding the sensor in this atmospheric window region, and thereby reducing the cloud effect. A further minimization of the cloud problem was achieved by offsetting the scan dither towards space. This was accomplished by biasing the track signal so that tracking occurred at a point where the field of view extended farther into space than into Earth during the dither. The tracking point was thus established well into the upper atmosphere where, for the spectral region used, clouds are not seen. Dynamic testing in which simulated clouds drifted through the field of view verified the approach, and subsequent flights have not experienced the problems of OGO 2.

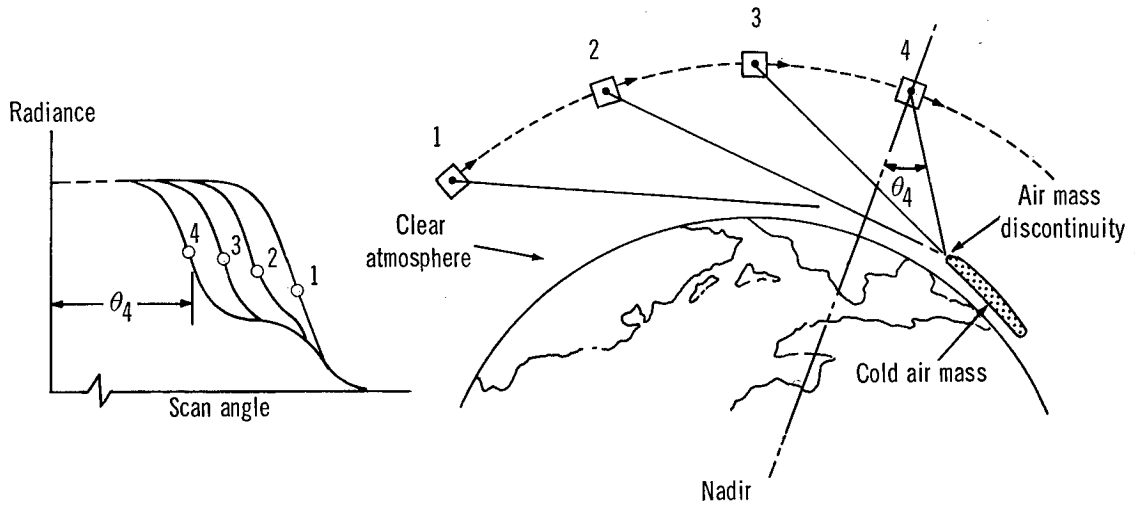

Figure 7.–Cloud-edge tracking.

The sensor heads were mounted with the scan plane angularly offset from the vehicle control planes to prevent the Sun from being directly in a scan plane; an offset of 1.6° (0.028 rad) was used. Subsequent analysis and testing during the optical redesign following the OGO 2 cloud problem showed that when the Sun was between 1.2° and 3.5° from the scan plane, scattered sunlight and heating of the detector base by the solar image would produce signals smaller than the Sun alarm threshold but greater than the Earth horizon threshold. This signal could have been falsely interpreted as the Earth horizon signal. Thus the 1.6° angular offset of the scan plane from the expected Sun line placed the scan plane directly in the dangerous region where Sun tracking without Sun alarm would occur creating a potential gas depletion problem, as in OGO 2. The offset was further increased to 5.8° and the problem was avoided.

A similar problem was uncovered on OGO 4, but in this instance the spurious tracking was caused by moonrise. One head locked onto the rising, illuminated Moon, causing a large attitude error in one axis. Fortunately, the reaction jets had been disabled at the time the error existed and the vehicle did not track the Moon. The solution to the problem is to predict the potential Moon interference occasions and to disable the reaction jets during those times. The OGO sensor history is summarized in reference 13.

Historically, little was known about the Earth scene at the time, although the problem is well understood today. Flight experience demonstrated that better knowledge of the spectral and spatial radiance distribution of the Earth was needed during the design and that this knowledge should have been used in more extensive dynamic testing.

2.3.2 Gemini Sensor

The Gemini horizon-sensor development was plagued by problems nearly identical to those of OGO: mechanical failure under vibration, spectral region not selected to minimize cloud effects, and Sun tracking.

At the time of the initial design, the cloud problems experienced on the Mercury flights were known, and sufficient analysis of the problem had been made to realize that the 15-μm CO_2 absorption band was most probably the best spectral region for horizon sensing. There were, however, no available filters for this region. The next best choice, for which filters were available, was the 13.5-to-22-μm region, but these filters exhibited humidity-sensitive degradation and could not be used. The 8-to-22-μm region was finally selected as the best compromise. Flight experience showed that clouds and the Sun caused problems, but not of the same magnitude as in the Mercury flights. With the Sun as far as 10° away from the scan field, tracking errors and loss of horizon track were experienced. Horizon track was lost every time the Sun was near the horizon. This occurred 117 times. The sensor also tracked cold clouds that drifted through the sensor field of view. However, because the field of view scanned the horizon over 160° of azimuth instead of at a single point, clouds only caused an increase in output noise, rather than the large output errors experienced by Mercury and OGO. A nearly complete overcast would be required to cause continuous tracking of a cloud front.

Each Gemini spacecraft normally had an active sensor and an identical redundant sensor. However, on spacecraft 9, revised design techniques overcame the humidity problem and the spectral bandpass of the redundant sensor was from 13.5 to 22 μm rather than from 8 to 22 μm. Its performance could then be compared to the sensor in use which had the 8-to-22-μm bandpass. A qualitative analysis indicated superior performance for the narrower spectral band sensor with no observed losses of track or wandering outputs resulting from Sun or cloud effects.

EMI problems were uncovered during system integration tests. Successful sensor operation required changes to both the spacecraft and sensor:

(1) Shielding and filtering of the spacecraft wiring was increased.
(2) Spacecraft power supplies were redesigned to reduce starting transients.
(3) Transient suppression networks were added to the sensor.
(4) Demodulation was changed from half wave to full wave.
(5) The preamplifier was redesigned for an FET (field-effect transistor) input stage, which is more compatible with thermistor bolometer impedance.

Additional EMI protection could have been obtained by providing a separate, isolated bias supply for the detector and preamplifier.

2.4 Radiance-Balancing Sensors

Radiance-balancing sensors do not employ object-plane scanning of a detector field of view (as do the previously discussed wide-angle scanners and dithering edge trackers). The radiance balancing technique assumes that when a radiance balance is achieved, the sensor optical axis is pointing at the center of the illuminated or self-emitting Earth disk.

This type of sensor is embodied in a variety of forms. One such form consists of four individual detectors with large fields of view that cover much of the Earth. The outputs of the two detectors viewing opposite horizons are differenced to provide a signal proportional to Earth offset angle. A second form drives a small detector field of view to grazing incidence on the horizon. A third version utilizes an electronically scanned array of sensors and has no moving parts.

Radiance-balancing sensors are often designed to utilize the thermal discontinuity at the edge of an optically formed Earth image, without modulating the incoming energy. Consequently, the detectors employed may be thought of as strictly temperature sensors. Their output is a function of the temperature distribution of the image surface on which they are located. This temperature distribution is influenced not only by the flux density collected and focused by the optics but also by radiation and conduction from sources within the sensor itself. The detector cannot differentiate between temperature differentials caused by the image and those caused by the local environment of the sensor. Thus the primary design task is to assure that thermal gradients caused by the sensor's local environment are of a magnitude

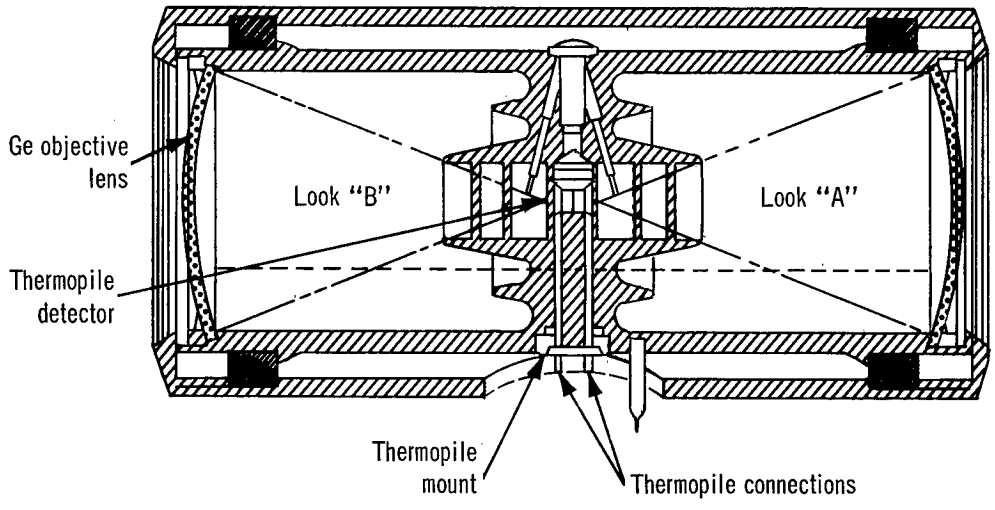

Figure 8.—Pegasus sensor.

sufficiently less than those caused by the Earth's image so that the required accuracy can be achieved.

Various techniques have been employed to obtain thermal uniformity. In the Pegasus sensor, which was used to define the approximate Earth direction for a tumbling vehicle, two thermopile detectors were mounted back to back so as to view object space in opposite directions through separate lenses, as illustrated in figure 8 (from ref. 15). The mechanical and optical design was made as nearly symmetrical as possible. Consequently, a difference in detector temperature could be expected to arise only from infrared sources outside the sensor. The detector dc output was modulated by a solid-state photomodulator to avoid the usual problems associated with dc amplifiers.

The Goddard Space Flight Center Reliable Earth Sensor (refs. 16 and 17) was developed for operation at synchronous orbit. This sensor was designed to image the Earth onto an array of eight metal bolometers arranged in a radial pattern, as shown in figure 9 (from ref. 16). Four of these bolometers are alined to vehicle axes and are the primary detectors; the other four are rotated 45° from the vehicle axes and are used either for redundance or for instances when the Sun is in the field of view of one of the primary detectors. Metal bolometers were selected over thermopiles because of their larger available signal voltage. The development of a suitable metal bolometer was, however, the most difficult problem encountered. The differential output of a metal bolometer bridge is a function not only of the detector temperature difference but also of the ambient temperature and the difference between detector time constants. To provide the required thermal stability and uniformity, the cavity between the lens and detectors was temperature controlled by a coil heater. Initial time constant mismatch was compensated by adjusting the mass of the mandrels supporting the platinum wire of the bolometer.

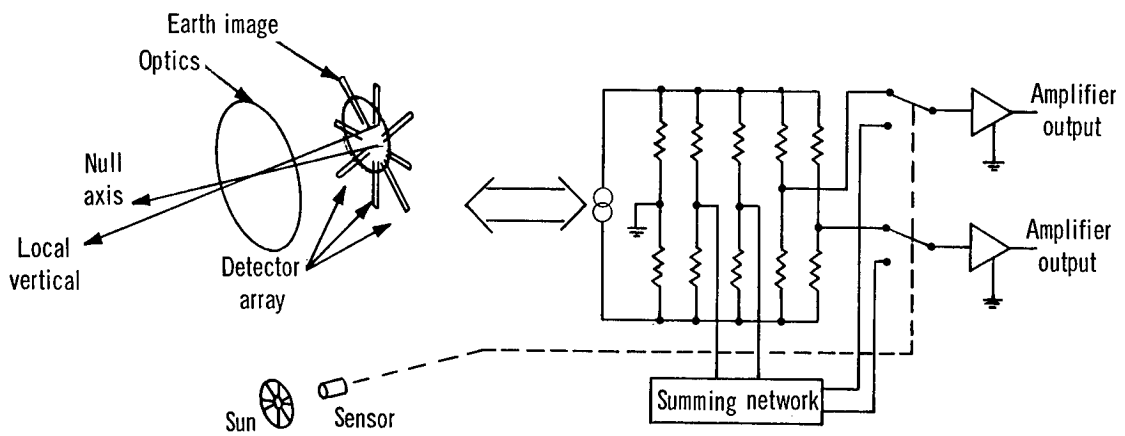

Figure 9.–Reliable Earth sensor.

Detectors for radiance-balancing sensors are limited to thermopiles and metal bolometers. Thermistor bolometers exhibit wide variations in resistance and responsivity and in the effects of ambient temperature on these parameters. The precise temperature control required to prevent mismatch in two balancing detectors makes the use of thermistors impractical (ref. 15).

Another factor that has to be considered when thermistor bolometers are used is thermal runaway. A thermistor bolometer changes its resistance with temperature. The thermistor material has a negative temperature coefficient. At a temperature called the detector critical temperature, the bolometer impedance has been reduced to the point that the high bias current causes detector self-heating and thermal runaway.

Thermistor bolometer behavior (ref. 18) for a detector biased at 60 percent of peak bias voltage and base temperature maintained at room ambient is as follows:

Detector signal/noise ratio	Behavior
10^1 to 10^5	Output is proportional to input.
10^5 to 10^6	Output is approximately proportional to input.
10^6 to 10^7	Output is not proportional to input.
10^8	Detector heating produces a large resistance and voltage imbalance in bolometer bridge.
10^9	Detector heating causes degradation of cements used in construction, and the detector burns out.

2.5 State of the Art Summary

Table I summarizes a number of sensor characteristics. Care must be exercised in interpreting this table because the best values given are not necessarily applicable to any one known sensor.

3. CRITERIA

Horizon sensors should be designed to indicate the angular position of the optical discontinuity, near where the Earth profile meets the space background, for determination of the spacecraft local vertical under all specified operational conditions.

The design should achieve required accuracy, lifetime, and reliability within imposed size, weight, and power constraints. The design shall minimize adverse effects of the natural

TABLE I.–*State of the Art Summary*

Characteristic	Possible choices or range of values	Principal factors involved
Sensor type	Conical scan Edge tracker Radiation balancing Horizon-crossing indicator	Accuracy required, operational altitude; length of mission; type of satellite, i.e., spinning or 3-axis stabilized; and degree of mechanical complexity permitted
Spectral band	CO_2 absorption band 14-16 μm H_2O absorption band 20-35 μm	Adequate signal/noise ratio for desired scan type, good cloud rejection, and horizon stability
Optical material	Germanium or silicon	Desired spectral band
Aperture	1 to 3 in.	Large enough to give adequate signal/noise ratio for selected spectral band and scan type
Field of view	0.75° to 3° rectangular, square, or circular	Accuracy required, must give adequate signal/noise ratio for selected spectral band
Accuracy	0.05° to 2°	Altitude of operation Spectral band selected Length of mission Degree of mechanical and electrical complexity permitted
Sun rejection	Use of separate detector Use of main detector by noting signal level, pulsewidth, etc.	Degree of complexity permitted Ability to anticipate Sun's presence before entering field of view
Detector type	Thermistor, metal bolometer, or thermopile	Selection depends mainly on type of sensor, whether scanning or nonscanning
Reliability	MTBF[a] = 15 000 hr to 120 yr	Accuracy required, weight and power limits
Weight	0.5 to 25 lb	Accuracy required, type of scan desired
Power	0.5 to 20 W	Accuracy required, type of scan desired

[a]Mean time between failures.

environment, including cold clouds, atmospheric scattering, Sun interference, Moon interference, and Earth radiance nonuniformities. Susceptibility to spacecraft adverse environmental effects including mechanical obscuration, electromagnetic interference, thermal radiation, and thermal conduction must be minimized. The output signals should be compatible in level, dynamic range, data rate, and format with the control system of which they are functional elements.

The simplest, most reliable design capable of performing the specified function should be provided. Designs developed with flight-proven hardware and techniques should be used whenever practicable.

3.1 Input Phenomena

3.1.1 Spectral Region

The spectral region of operation should be selected to be consistent with performance requirements, considering effects caused by clouds, Earth spatial and temporal temperature differences, and radiance profile shape variations.

3.1.2 Sun Interference

Detector damage by solar heating must be prevented. Output errors caused by the Sun being in or near the detector field of view shall be minimized. An alarm signal should be considered to indicate actual or impending Sun errors. This alarm signal should be compatible with switching logic circuits so that appropriate action may be taken consistent with the horizon-sensor design and the requirements of the spacecraft attitude-control system.

For radiance-balancing sensors, output errors and detector-plane thermal gradients must be considered when the Sun is in or near the total field of view encompassed by all detectors.

3.1.3. Internal Reflections

The optical design should be such that multiple reflections from external sources, such as the Sun, Moon, Earth, or spacecraft, and from sources within the sensor itself do not

generate spurious detector signals sufficient to cause output errors greater than a predetermined tolerable magnitude.

3.1.4 Moon Interference

Effects of Moon interference shall be analyzed and considered. Moon interference effects on the horizon-sensor output and the influence of the erroneous output on the spacecraft mission should be considered.

3.2 Design Interfaces

The following factors, derived from vehicle system and operational interfaces, shall be considered in the design and by the user.

3.2.1 Optical Interface

The optical interface with the spacecraft must be designed so that no part of the spacecraft or its appendages can appear in the field of view of the sensor or be close enough to the field of view to cause output errors. Alternatively, the sensor must contain sufficient logic to reject spurious signals if the field of view of the sensor must include part of the spacecraft, expended reaction jet fuel, or jettisoned parts.

3.2.2 Electrical Interface

Control shall be imposed on the electrical interface with the spacecraft to prevent spurious signal and noise inputs to the detector preamplifier. The prevention of electromagnetic interference is vitally important because of the low signal levels usually encountered in horizon sensors.

3.2.3 Thermal Interface

The thermal design must include special considerations of the radiant thermal interface defined by radiative inputs from Sun, Earth, space, and spacecraft in addition to the normal thermal-conduction interface with the spacecraft, because of the exceptional thermal sensitivity of all types of sensors.

3.3 Other Design Considerations

3.3.1 Scan Mechanization Protection

Sensor designs that use gears and/or bearings that require lubrication must be provided with reliable seals. The optical elements must be protected from contamination by evaporated lubricant, whether from seal failure or other causes. Sensors with torsional-suspension scanning elements, e.g., flex-pivot or taut-wire suspension, must be adequately protected from the launch environment. Fatigue in flex pivots must be considered.

3.3.2 Thermal Design

For sensors using thermistor bolometer detectors, safeguards must be included to prevent thermal runaway of the detector. For radiance-balancing sensors, the thermal design must consider the effects of output errors caused by temperature gradients across individual detectors, thermal gradients between detectors, and the temperature range over which the detectors shall operate.

3.3.3 Detector Life

The thermal environment of detectors, especially immersed thermistor bolometers, should be consistent with required operating time and life versus temperature characteristics of the detectors.

3.3.4 Alinement Provisions

Means for alining the sensor to the required spacecraft references and for verifying this alinement after installation on the spacecraft shall be provided in the design.

3.3.5 Contamination and Degradation of Optical Elements

Contamination and degradation of internal and external optical elements must be prevented. If dust covers are used, positive dust cover removal procedure shall be provided. In all phases of design, including the specification of assembly, test, and handling procedures, attention must be given to the prevention of degradation of any optical element or surface. This includes prevention of contamination during fabrication and testing as well as during mission orbit.

3.3.6 Corona Suppression

The design shall prevent the occurrence of corona discharge at all specified ranges of temperature and pressure. Any electrical potentials above approximately 100 V should be suspect. The low pressure of orbit shall not be depended upon to prevent discharge because of the contingency of accidental turn-on before outgassing is complete.

3.4 Performance

3.4.1 Acquisition

The sensor design must provide the required probability of initial Earth acquisition. Loss of track resulting from variations in apparent Earth diameter over the expected mission altitude range and over the required range of vehicle attitudes must be prevented. Alarms to indicate loss of track and/or automatic reacquisition sequence if track is lost should be considered.

3.4.2 Performance Tests

In addition to tests conducted to verify sensor performance, the test plan should specify that each sensor be subjected to at least one field of view test over the dynamic range of expected radiant inputs and to a cold-wall test with the sensor operated over its expected environment.

3.4.3 Launch-Site Checkout

Required launch-site performance testing should be defined early in the design phase.

4. RECOMMENDED PRACTICES

The selection or design of an Earth horizon sensor for a particular application involves a complex tradeoff between altitude range of operation, accuracy, reliability, size, weight, power, and cost. The user's requirements for operational altitude, linearity, and cross coupling will dictate the scan pattern. The specifications on accuracy and response to spurious signals from cold clouds and the Sun will govern the spectral band, aperture, and field of view. The size, weight, and environment will influence the lenses, mirrors, and material selection. The environment and life requirements will affect the choice of rotational or dither rate, construction, and alinement.

Within the broad infrared spectrum of 2 to 30 μm, the Earth presents a variety of horizon scenes, depending on the specific portion of the spectrum used. Where accuracy is limited by horizon noise, the preferred spectral region is the 15-μm CO_2 absorption band embracing the spectral region from about 14 to 16 μm—although the mechanization employed may include radiation of longer wavelengths.

If lifetime and reliability are primary requirements, a static (i.e., no moving parts) sensor is indicated. However, accuracy may dictate the need for dynamic scanning or tracking. Design approaches for dynamic scanning devices range from sealed units with gears and bearings to units with no metal-to-metal friction.

Early plans for appropriate spacecraft performance tests and launch-site checks should be made. Detailed plans should provide for avoiding Sun and Moon interference, thermal runaway, optical ghosts, and EMI.

4.1 Input Phenomena

4.1.1 Spectral Region

The selection of the spectral region of operation is a most important step in the design process and is based on a tradeoff that is influenced by many factors, the most important of which are the properties of the horizon radiation, the Sun's radiation, and the available components.

The correct spectral region for a particular sensor depends greatly on orbit parameters and scan pattern, and represents the best achievable compromise between accuracy and volume.

Operation at wavelengths shorter than about 12.5 μm is to be avoided if possible. The optimum spectral region for high accuracy is the 15-μm CO_2 band from about 14 to 16 μm. For cases where lower accuracy can be tolerated, the 12.5-to-40-μm region may be more advantageous.

4.1.1.1 Earth Spectral Distribution

The Earth-emitted spectral distribution is given in figure 10 (from ref. 1). These approximate curves, which should be considered as illustrative of the Earth's spectrum rather than as hard design data, show that the Earth radiates significantly only at wavelengths greater than about 6 μm.

The spectral distribution of reflected solar radiation is contrasted with blackbody distributions comparable to the Earth's spectral radiance in figure 11 (from ref. 19). Below 5 μm the reflected solar radiation is much greater than self-emitted Earth radiation. Thus a sensor field of view scanning across a partially illuminated Earth would see three large gradients, one at each limb and one at the terminator, if its spectral response extends below 5 μm. The gradient at the terminator could be misinterpreted as the horizon unless the sensor signal processing (or ground data reduction, where applicable) compensates for this error.

Sensors with a response below 6 μm have to be designed to eliminate erroneous signals caused by reflected solar radiation.

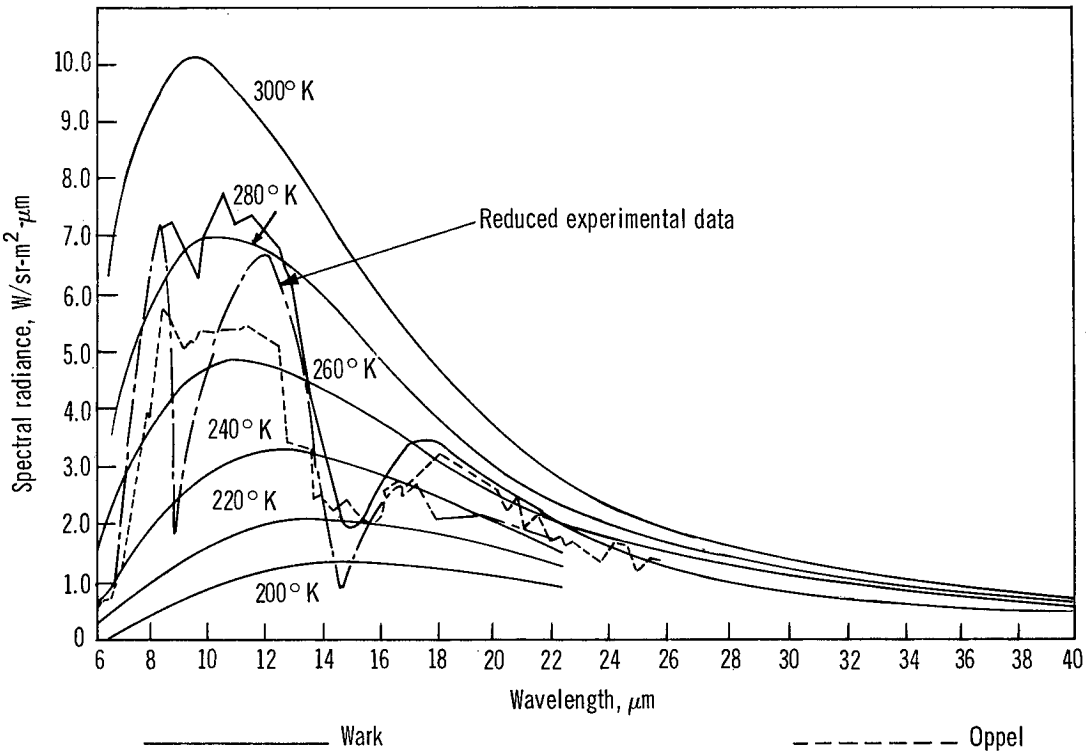

Figure 10.—Comparison of estimated and measured upwelling radiation, temperate atmosphere, and vertical path.

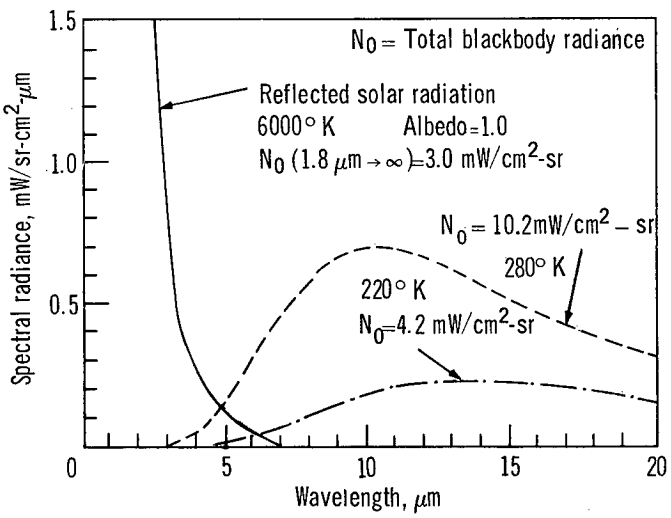

Figure 11.—Reflected solar and simulated Earth blackbody/ spectral energy/distribution curves.

4.1.1.2 Horizon Stability

In those applications where high accuracy is required, a spectral region should be selected to minimize the angular instability of the horizon. The 15-μm CO_2 band satisfies these objectives; the specific spectral width with best stability encompassing this band was shown in reference 20 to extend from 14.0 to 16.3 μm, with potential detected horizon stability better than 1 km. The radiance profile in that spectral band exhibits deterministic variations with time and latitude as well as random variations. The deterministic changes have been demonstrated analytically and verified experimentally as shown in references 21 through 24. For missions in which extreme accuracy is required, programed compensation for the deterministic effects can improve the local vertical accuracy as indicated in reference 25. For other spectral regions, horizon profiles can be generated from data in reference 26 to assess the effects of atmospheric changes.

In addition, amplitude effects can be compensated for by normalizing the time-varying detector output signal to the measured peak radiance or peak detector signal. This has the effect of producing what have been called normalized radiance profiles (refs. 1, 27, and 28). The radiance amplitude effects can be eliminated as shown in figure 12 (from ref. 9). However, care must be taken that the spectral region selected does not allow the radiance compensation technique to be confused by atmospheric anomalies.

4.1.1.3 Horizon Detection

As a detector field of view sweeps across the discontinuity between Earth and space, it generates an output signal that is a function of the magnitude and shape of the limb radiance profile, as distorted by the transfer function of the sensor. The relationship between the defined infrared horizon and the hard Earth horizon depends on the detection technique used.

A fixed threshold on the detector signal is shown in reference 28 to be one of the more stable techniques. Other features of the detector waveform can be used for horizon identification. Techniques such as sensing a particular value of slope or the waveform inflection point, or extrapolation of the linear portion of the waveform to zero signal on the time or scan angle axis may be employed. However, these techniques require more complex electronics than simple threshold sensing and might offer advantages only in certain special instances. References 1, 27, and 28 discuss many of these signal-processing techniques and their related accuracies. References 29 to 36 provide additional data regarding Earth horizon characteristics that affect the horizon detection problem.

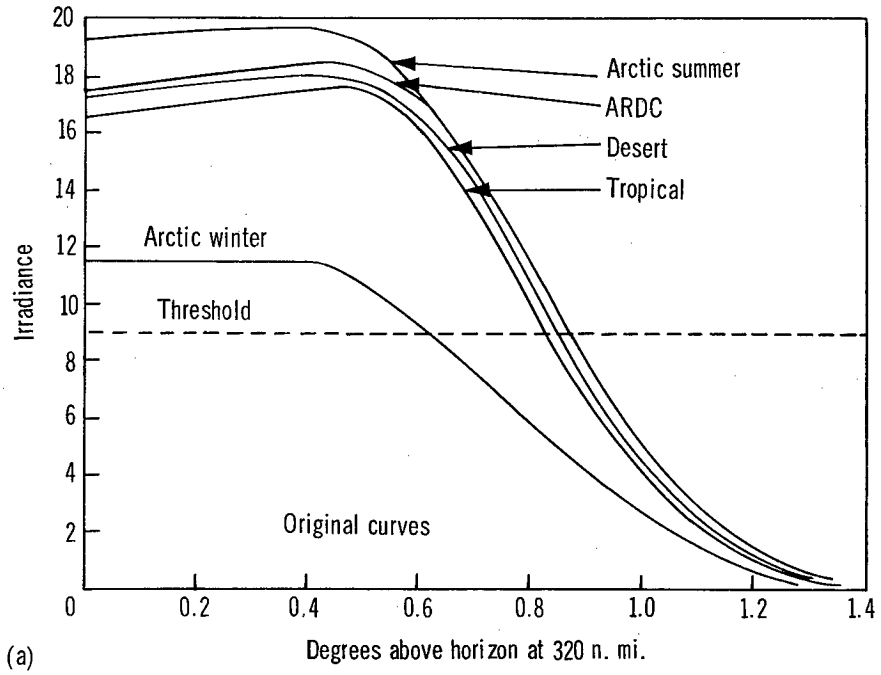

(a)

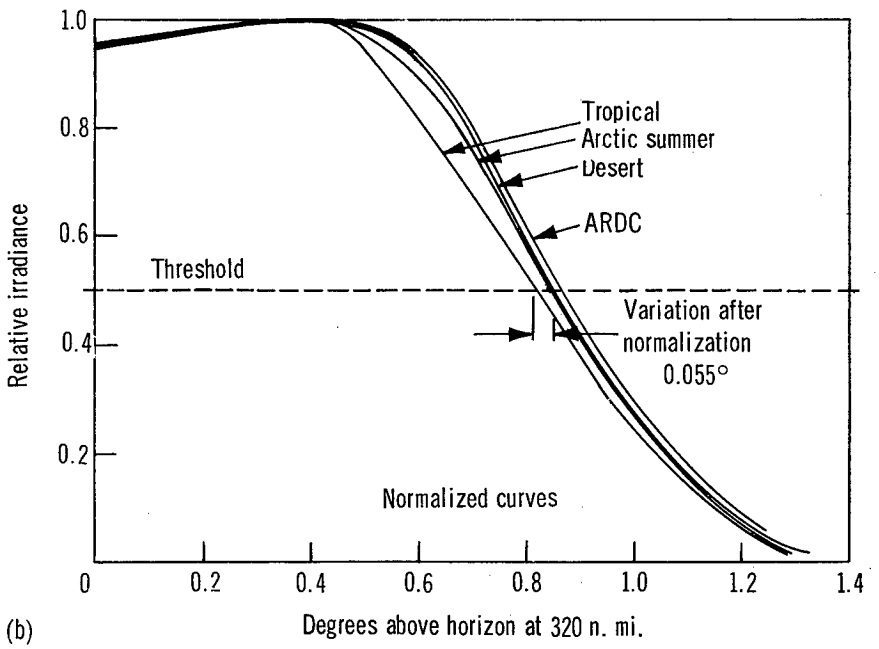

(b)

Figure 12.–(a) CO_2 band horizon profiles. (b) CO_2 band horizon profiles, normalized.

4.1.2 Sun Effects

The two primary Sun effects to be considered are detector damage in sensors using thermistor bolometers that are not adequately shielded, and output errors, which exist even when adequate protection is provided.

4.1.2.1 Detector Damage

Thermistor bolometers can reach a critical temperature where the bolometer impedance has been reduced to the point that the resulting bias current causes detector self-heating and thermal runaway.

Care must be taken that the sum of the temperature rises caused by the radiation of the Sun and the operating temperature of the sensor does not exceed the detector critical temperature.

Thus, in any particular application using thermistor bolometers, detector heating by the Sun must be carefully analyzed to determine potential detector damage. The margin of safety can be increased by narrowing the spectral region, by decreasing the temperature of the detector heat sink, and by operating the detector at less than the recommended 60 percent of peak bias. If these steps do not provide sufficient safety margin, a Sun shutter may be used to block the optical path until the Sun is no longer in the field of view, or a vehicle maneuver can be executed to change the sensor/Sun line of sight while still maintaining adequate sensor/Earth geometry to retain sensor function.

Thermopile detectors do not exhibit the thermal self-heating from bias currents that affect thermistor bolometers. They would not be damaged until incident radiation caused the detector to reach the sintering temperature of the detector materials or the softening temperature of the backing materials.

4.1.2.2 Output Errors

When the Sun is in or near, in some instances, the detector field of view, detector output will confuse the sensor signal processing unless some form of discrimination exists. Discrimination is based on amplitude sensing, pulsewidth logic, separate Sun sensing detectors, or a combination of these.

When the Sun is in such a position relative to the horizon and to the detector field of view that amplitude discrimination and pulsewidth discrimination are not effective, one of the following steps can be taken:

(1) The resulting pointing error may be accepted.
(2) The sensor field of view can be caused to change its relative Earth/Sun orientation by a vehicle maneuver or by reorienting the scan planes within the sensor.
(3) A redundant sensor head or detector field of view can be placed into operation, as in the OGO sensor (ref. 13).
(4) The sensor output can be inhibited until the Sun problem is eliminated by the changing orbit position of the vehicle.

If a separate Sun detector is used to sense actual or impending solar interference, the output of the Sun detector must be sufficiently related to the Earth sensor field of view so that the critical Earth-Sun field-of-view orientation can be determined. When the Sun is on the horizon, atmospheric attenuation may prohibit sensing of solar interference by a separate Sun detector. In that case, if resulting horizon-sensor output errors must be avoided, the situation must be predicted and steps (2) or (3) above used.

The solar image presents a considerable thermal gradient problem to static or radiance-balancing sensors. This problem can be minimized by operating in as longwave a spectral region as possible to reduce the effective solar signal. Placement of the spectral filter outside the collecting aperture of the optics minimizes the amount of solar flux entering the sensor aperture and the asymmetric solar heating of the collecting optics and lens barrel (ref. 16).

Aside from these general statements, specific practices are too intimately related to sensor design details to be generalized. Exceptional optical and thermal design practices must be observed and the internal solar heating problem must be considered carefully.

4.1.2.3 Sun Rejection

The ratio of Earth spectral radiance to Sun spectral radiance using the data of figure 10 for the Earth and a 6000° K blackbody for the Sun, is illustrated in figure 13. Note that the Sun radiates about 2000 times as much as the Earth at the shortest wavelength at which there is significant Earth emittance, (i.e., 8 μm). Thus, a small field of view detector (less than 0.5° X 0.5° or 7.61 X 10^{-6} sr) with a spectral response centered at about 8 μm would receive a signal 2000 times greater than the Earth signal for which it was designed, when scanning across the Sun. The curve in figure 13 shows that operating at the longest possible wavelength minimizes the problem, and that the Sun radiates considerably more than the Earth, regardless of the infrared spectral region.

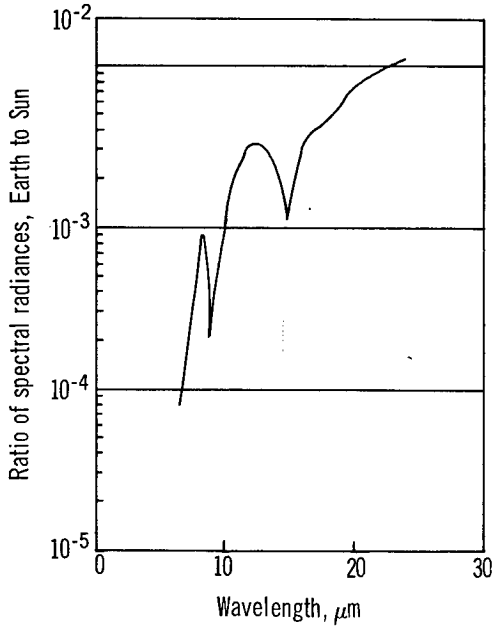

Figure 13.—Ratio of Earth spectral radiance to Sun spectral radiance.

By eliminating requirements for spectral filtering other than that provided by the inherent spectral transmission of the sensor optical materials, overall optical efficiency can be improved. Increased efficiency leads to a greater signal-to-noise ratio or a smaller aperture diameter, and consequently smaller overall size. Thus, if sensor operation and required accuracy permit, spectral response down to about 2 μm is permissible as in the Tiros horizon-crossing indicator (HCI) of reference 9.

The large Sun-to-Earth radiance ratio causes more problems when changing from the Tiros HCI-type sensor, to wide-angle mechanical sensors, or to dithering edge trackers. This ratio has the largest effect on nondithering, nonmechanical-scanning sensors (e.g., electronic-scan, wide-angle scanners or radiance-balancing sensors, or any sensor in which the detector field of view is relatively stationary in object space). As much sunlight as possible must be filtered out to prevent detector damage when the solar image is directly on the detector and to minimize thermal gradients across the detector planes, which cause output errors (refs. 11 and 17). The required magnitude of solar rejection depends on mission requirements and sensor type. The only guidelines on spectral region is that where stringent solar rejection requirements exist, filtering must be incorporated to limit the sensor spectral response to the longer wavelengths.

4.1.3 Internal Reflections

Improper control of internal reflections can cause ghost images of the Sun, and such solar ghost images can produce spurious detector signals. The unwanted internal reflections occur whenever refracting optical elements, such as lenses, are used. Unwanted reflections are suppressed through the use of thin film antireflection coatings on the offending refractive surfaces. Where possible, reflecting optics can be used in place of the refracting element. The number of refracting surfaces should be minimized and proper employment of light baffles and optical stops is important. Both geometrical optics and physical optics must be considered in the design. The optical design must be given an operational test in a cold-wall test chamber at the proper signal levels before the design can be considered adequate.

4.1.4 Moon Interference

If the field of view of the sensor scans across the Moon, the detector output signal will be a function of the lunar illumination phase—sometimes exceeding Earth threshold for a detector with a small field of view. These lunar signals can be discriminated against by measuring signal pulsewidth when the Moon is far enough from the horizon to produce a complete pulse. There will be times, however, when the Moon is so close to the horizon and the sensor field of view that it cannot be discriminated and a pointing error will result. Edge-tracking sensors are particularly susceptible to large errors during moonrise. The courses of action are the same as those listed in section 4.2 for Sun near the horizon.

Lunar interference can be eliminated by increasing the detector field of view. As the field of view increases beyond the angular subtense of the Moon, the detector signal from Earth increases but the lunar signal remains constant. However, use of a large field of view must be carefully evaluated with respect to other considerations, primarily accuracy.

The best-known method for determining when the Moon is in a location to cause interference is prediction based on the spacecraft orbital parameters.

4.2 Design Interfaces

4.2.1 Optical Interface

The horizon sensor responds to all the reflected and emitted radiation in its environment. Optical interface is defined to be the total optical environment of the sensor as it is mounted

on the orbiting spacecraft or during preflight testing. Both the user and the sensor designer must give detailed and careful thought to the optical interface between the horizon sensor and the spacecraft. No part of the spacecraft shall occupy any portion of the total field of view of the sensor. This restriction should apply even in the situations where some other part or function of the spacecraft fails.

Because it is not always possible to eliminate all potential field of view interferences, a secondary mode of operation should be designed. An example of such a mode is the gating off at certain times of the detector preamplifier in scanning sensors to avoid the offending obscuration or interference. In other situations it may be appropriate to recalibrate the sensor. Such a recalibration would be especially appropriate for a radiance-balancing type of sensor.

Space debris can adversely influence the operation of a horizon sensor. Such things as spent rocket stages and jettisoned parts or equipment, which do not leave the vicinity of the spacecraft, as well as particulate matter and gases from control jets or maneuver engines can temporarily or permanently degrade the accuracy of both radiance-balancing and scanning-type horizon sensors. The spacecraft designer and the sensor designer should jointly consider these possibilities.

4.2.2 Electrical Interface

Special attention must be paid to minimizing electrical interference in horizon sensors. The low signal levels and high detector impedances encountered in typical sensors make such attention mandatory; because thermistor bolometers used in most horizon sensors have impedances ranging from 2.5×10^5 to 2.5×10^6 ohms with signal levels of about 10^{-6} V, even a small amount of noise coupled into the detector can degrade the signal.

Conducted and radiated noise must be considered. Conducted electrical interference may be minimized by using a distinct detector bias supply and by properly isolating the power supplied by the spacecraft for other horizon-sensor functions. Radiated EMI must be controlled by a hard and realistic EMI interface plan that will identify the proper shielding and positioning requirements. While such actions are normal practice in most space programs, they must be given extraordinary consideration with horizon sensors.

4.2.3 Thermal Interface

The exact thermal interface problems to be solved in the design of a horizon sensor depend on the mission, spacecraft design, and the type of sensor to be used. Solar heating is by far

the greatest problem, and if the use of thermistor bolometer detectors is contemplated, they must be given adequate heat sinking and optical protection. The location of the sensor and the temperature of the spacecraft mounting member must be known before an adequate design of a radiance-balancing horizon sensor can be accomplished.

The use of a thermal-analysis computer program is strongly recommended for thermal interface design. The program should include all important thermal sources and sinks, and both conductive and radiative thermal exchange should be considered. The use of mechanical cooling, such as compressor-type refrigerators, is to be avoided. Other forms of active cooling, such as the use of Peltier coolers, are to be avoided wherever possible because of their power consumption.

The detailed interface design should be a joint effort by the spacecraft design team and the horizon-sensor designer. Continuous close liaison is essential to success.

4.3 Other Design Considerations

4.3.1 Scan Mechanization Protection

Low-frequency flexural pivots are preferred for small amplitude scans because such pivots require no lubrication and their reliability is high when they are properly designed. If large amplitude scans are required, a rotating bearing may be needed. In such instances the use of silicone-type seals is mandatory to prevent the loss of lubricant from the bearing. Dry-type bearings should be considered. Space-qualified seals and bearings are available and these should be used in the design wherever possible. The launch environment must be considered and the scan mechanism should be tested to adequate margin limits to assure survival during launch. In new mechanical designs where new techniques or novel elements are used, adequate life tests in vacuum environment should be run to establish the feasibility of the new design or technique.

4.3.2 Thermal Design

The thermal design of the horizon sensor is of critical importance. It cannot be separated from the thermal interface design of the sensor with the spacecraft and its mission. The

use of thermal-analysis computer programs and other computational aids is strongly recommended. Greatest emphasis should be placed on thermal protection of thermal-type detectors, such as thermistor bolometers. The principle of thermal symmetry should be used in the thermal design of radiance-balancing-type horizon sensors because thermal detectors are usually used and thermal imbalances cause output errors. During the mechanical and structural design of the horizon sensor, the thermal properties of a material should be considered of equal importance with the mechanical properties.

4.3.3 Detector Life

Because thermopile detectors do not suffer from the thermal self-heating problems of thermistor bolometers, they should be considered whenever solar heating is likely to be a problem. In horizon-crossing indicators, which work at shorter wavelengths, it is possible to choose from a wider variety of detector types. The use of deposited lead salt photoconductive detectors is not recommended because the longest wavelength to which these detectors are responsive is 6μm, and they are subject to damage in radiation environments, such as the Van Allen belt. If operation in a radiation environment is contemplated, either a thermopile or an intrinsic photoconductor should be used because these detectors are highly resistant to radiation damage.

4.3.4 Alinement Provisions

It is necessary to include provision for sensor alinement on the sensor itself. The most convenient form of alinement is the use of precision machined surfaces for mounting the sensor on the spacecraft. When the sensor is gimbaled or scans internally, the alinement procedure should include dynamic as well as static tests. Consideration of alinement of the sensor to test simulators and other optical devices should be made early in the mechanical design. The use of special alinement and test hoods that fit over the sensor aperture is often convenient. Such hoods can protect the sensor from contamination during testing, and when operated they can serve as an alinement check or a function check, depending on their specific design. Most horizon sensors operate in the infrared; the usual optical alinement tools will not be sufficient if there are any transmitting optical elements that are opaque to visible light. Optical alinement should, therefore, be considered early in the optical design. The use of a properly attenuated CO_2 laser is recommended, provided there are no elements opaque to 10.6-μm radiation. If possible, the instrument should be alined with the opaque elements (filters) removed.

4.3.5 Contamination and Degradation of Optical Elements

Certain glasses darken or yellow upon exposure to ionizing radiation. For the shorter wavelengths, therefore, the use of fused silica is recommended. Infrared elements for lenses and filter substrates must be chosen with care also. Germanium and silicon must be of very high purity or scattering will occur at infrared wavelengths even before exposure to ionizing radiation. The radiation will aggravate the scattering, and the effect is cumulative with time in orbit.

Properly coated mirrors are highly resistant to degradation, but the protective coating must be applied uniformly. The rate of sublimation of the coating material must be considered. The mirrors must be protected from organic and other contaminants originating from several sources. Rocket fuel, control jet fuel, horizon-sensor bearing lubricant, and subliming or evaporating constituents of paints and organic coatings within the sensor are typical sources. Recommended practice is to use only space-proven paints and finishes. Any new coating or paint should be given a life test for change of weight under vacuum environment at the expected temperatures. Where possible, objective lenses can serve as a protective window for other optical elements. Entirely reflective optical systems are more difficult to protect. Recommended practice in such windowless systems is to keep a protective cover in place during testing and checkout and to remove the cover as late as possible.

4.3.6 Corona Suppression

Corona suppression is best achieved by avoiding the use of high voltages in the sensor. Also, it is necessary to avoid any sharp pointed terminals or other electrical conducting metallic parts because electrostatic fields are stronger in regions where the radius of curvature is very small. The most common source of sharp points in electrical circuit boards is improper soldering. Proper inspection is, therefore, required. The use of sharp edges and corners should be avoided in the mechanical design of the electrical conductors. Another source of corona is found in improperly impregnated connectors, cables, transformers, and chokes where small voids in the impregnant act as corona centers. The recommended practice is to use a very high vacuum when impregnating such units. Corona specifications should be imposed on transformer manufacturers, and the appropriate specifications should be utilized in specifying corona and the testing for same. In unpotted shielded cables it is possible to obtain corona from trapped air or gas pockets in multiwrapped insulation. The recommended practice is to provide sufficient time for outgassing before commencing operating or testing.

4.4 Performance

4.4.1 Acquisition

The total field of view of the sensor should be sufficiently large to allow Earth acquisition under worst expected attitude-error conditions. The sensor should indicate loss of track to the attitude-control system to avoid expenditure of attitude-control fuel.

Automatic reacquisition should be considered; however, close cooperation with the attitude-control system design team is required to insure system compatibility during loss of track.

4.4.2 Performance Tests

The horizon-sensor system is part of an overall spacecraft system, and should be tested as part of the spacecraft. When testing at the spacecraft level is not possible, a complete series of laboratory tests is required. They should include response to a simulated horizon gradient, exposure of the sensor to the radiant background, exposure of the detector to its thermal environment, system linearity and accuracy, optomechanical alinement with the spacecraft, geometric effects the sensor and spacecraft together may have, and EMI effects upon and by the sensor.

The simulated horizon gradient must include both the radiance level of the space background (4° K) and the Earth (300° K), and the transition of one to the other—usually in a nonlinear way. But even in a space chamber, exact simulation of the space background at 4° K is all but impossible. Fortunately, all that is required of the simulated space background is that its radiance be less than the equivalent radiance of the sensor noise level, or well below simulated Earth radiance. A liquid-nitrogen (77° K) cooled blackbody background would have a radiance at least 50 times less than that of the minimum Earth temperature, and can simulate the space background satisfactorily. Performance tests in a vacuum chamber against a simulated Earth with a radiance equivalent to the actual Earth radiance in the sensor spectral region and with liquid-nitrogen or colder background temperature should be conducted on the complete sensor design to check both for accuracy and responsivity, and for absence of multiple internal reflections. During tests of this type, the Earth, Sun, and space radiances should be tested simultaneously so that effects of the Sun near the horizon may be evaluated. (These usually are scattering and multiple internal reflections.) During such testing the flux transmitted to the detector from the simulated Earth and Sun must be comparable to that from the actual Earth and Sun. This can be achieved with practical temperatures by changing the spectral acceptance of the sensor.

Most system tests, i.e., accuracy, linearity, and acquisition, need not be run in a vacuum chamber but can be run at laboratory ambient conditions. For such tests, a background with uniform radiance at the temperature of the room can be used to simulate space. The simulated Earth target has to be at an elevated temperature such that the difference in radiance between target and background in the sensor spectral region is equivalent to Earth horizon radiance. For example, the radiance difference between a 300° K blackbody background and a 330° K blackbody target is about 5 W/m^2-sr in the 14-to-16-μm region, about the same as nominal Earth radiance. In practice, backgrounds and targets are not blackbodies but have an emissivity that is a function of wavelength. Target spectral radiance and background spectral radiance must be integrated over the spectral response of the horizon sensor, with target and background temperature differences being adjusted until the following equation is satisfied:

$$N_h = \int N_e(T,\lambda)\epsilon_e(T,\lambda)\tau(\lambda)R(\lambda)\,d\lambda - \int N_b(T,\lambda)\epsilon_b(T,\lambda)\tau(\lambda)R(\lambda)\,d\lambda$$

where

N_h = simulated horizon radiance
N_e = simulated Earth radiance
N_b = simulated background
$N(T,\lambda)$ = blackbody spectral radiance; Planck's function
$\epsilon(T,\lambda)$ = spectral emissivity, often a function of temperature as well
$\tau(\lambda)$ = atmospheric spectral transmission over the optical path
$R(\lambda)$ = sensor spectral response (both optics and detector have to be considered)

For either cold wall or ambient performance testing, the geometric relationships of the test setup must be carefully considered and controlled. In actual operation, the Earth horizon is at infinity relative to the sensor optics and the sensor is always on a perpendicular line through the center of the Earth disk—regardless of spacecraft orientation. In the laboratory, the simulated horizon is not at infinity and the horizon image could be blurred by defocusing. This could produce a detector output sufficiently different from that produced by the actual horizon to negate any test results. In some cases, the magnitude of defocusing can be controlled so that the blurred image of the sharp-edged simulator closely approximates the image of the horizon radiance profile. If this is not the case, the focusing problem can be handled by using a collimator to make the simulated horizon appear to be at infinity (ref. 21) or by refocusing the detector for the proper target-sensor distance.

In these laboratory tests, the sensor may not be on a perpendicular line through the center of the simulated Earth disk. If the sensor is mounted on a rotary table to provide sensor angular motion relative to the horizon, a certain amount of translation occurs, and this is equivalent to further angular motion with a relatively short sensor-target distance. The true rotation of the sensor relative to the simulated local vertical is the combination of sensor rotation and translation-induced rotation, and must be computed to eliminate a source of

test error. Alternatively, the translation-induced error can be reduced by always recentering the sensor after a sensor rotation. Reference 29 describes horizon simulators in which the geometry of the simulator is changed to provide simulated angular motion without rotating the sensor, thereby minimizing the translation problem.

4.4.3 Launch-Site Checkout

The testing of horizon sensors after they are part of a spacecraft system can sometimes be exceedingly difficult. The illumination of the sensor with the proper horizon and background sources is the chief problem. The designer should consider early in the design process how he will accomplish this task, especially at the launch site. It may be satisfactory to establish only whether or not the system operates; however, more exacting tests may be necessary. The minimum test sequence should include an optical and electronic function test. It may be necessary to employ an electronic performance test with simulated detector output signals, and an optical performance test that uses an accurate and appropriate partial or full-scale simulation of the actual background and horizon gradient actuating the control system of the spacecraft. This list is given in the order of difficulty and completeness. The designer and user must decide early in his program which test level is required, and plan for it appropriately.

The simulation of optical tests is the most difficult. One solution is to provide test gear which can be attached directly to the sensor. Electronic test signals are easier to insert, but test points and special connectors must be considered. The test signals should be designed to verify as much system performance as is possible. Angular alinement of the sensor to the spacecraft has to be checked. If complete simulation at the spacecraft level is not performed, one or two mirrors should be mounted in the sensor to allow alinement verification.

REFERENCES

1. Duncan, John; Wolfe, William; Oppel, George; and Burn, James: Infrared Horizon Sensors. Rept. no. 2389-80-T, IRIA State-of-the-Art Report, Inst. of Sci. and Technol., Univ. of Michigan. NAVSO P-2481, Apr. 1965. (Also available as AD-466-289.)

2. Astheimer, Robert W.: Infrared Horizon Sensors for Attitude Determination. Paper presented at IFAC Symposium on Automatic Control in the Peaceful Uses of Space (Norway), 1965.

3. Lunde, Barbara K.: Horizon Sensing for Attitude Determination. Paper presented at Am. Astronaut. Soc., Goddard Memorial Symposium (Washington, D.C.), Mar. 16-17, 1962. NASA-GSFC no. 62-47.

4. Spielberger, Seymour C.: Conical Scan Horizon Sensors. Proceedings of the First Symposium on Infrared Sensors for Spacecraft Guidance and Control, Barnes Engineering Co. (Stamford, Conn.), May 1965.

5. Wolfers, C. V.; and Motcham, H. L.: Mercury/Gemini Program Design Survey. NASA CR-86011 (McDonnell Douglas Rept. F917, NAS 12-586), Jan. 31, 1968.

6. Wolfe, William L.; and Duncan, John: Immersion Lenses for Infrared Instruments. Proceedings of the Conference on Optical Instruments and Techniques, Chapman and Hall, Ltd. (London), 1962, pp. 297-304.

7. Astheimer, R. W.; DeWaard, R.; and Jackson, E. A.: Infrared Radiometric Instruments on TIROS II. J. Opt. Soc. Am., vol. 51, no. 12, Dec. 1961, pp. 1386-1393.

8. Horan, John J.: Performance and Systems Applications of Horizon Sensors for Spin Stabilized Spacecraft. Proceedings of the First Symposium on Infrared Sensors for Spacecraft Guidance and Control, Barnes Engineering Co. (Stamford, Conn.), May 1965.

9. Arck, Morris, H.: Horizon Sensors for Spin Stabilized Spacecraft. Proceedings of the First Symposium on Infrared Sensors for Spacecraft Guidance and Control, Barnes Engineering Co. (Stamford, Conn.), May 1965.

10. Merlen, Monroe M.; Pasternak, Jerome M.; and Pearsall, Denton: An Electronic Scan Horizon Sensor. Proceedings of the First Symposium on Infrared Sensors for Spacecraft Guidance and Control, Barnes Engineering Co. (Stamford, Conn.), May 1965.

11. Caveney, Robert D.: Second-Harmonic Edge-Tracker Horizon Sensor, Fixed-Point Type. Proceedings of the First Symposium on Infrared Sensors for Spacecraft Guidance and Control, Barnes Engineering Co. (Stamford, Conn.), May 1965.

12. Morales, Eleazer W.: Second Harmonic Edge Tracker Horizon Sensor—Azimuth Scanning Type. Proceedings of the First Symposium on Infrared Sensors for Spacecraft Guidance and Control, Barnes Engineering Co. (Stamford, Conn.), May 1965.

13. McKenna, K. J.; and Schmeichel, H.: Orbiting Geophysical Observatory Attitude Control Subsystem Design Survey. NASA CR-86107 (TRW, NAS 12-110), June 28, 1968.

14. Weiner, R. M.; and Gonzales, L: Earth Model for Design and Evaluation of Edge-Tracking Earth Sensors. Paper presented at the Second Symposium on Infrared Sensors for Spacecraft Guidance and Control, Aerospace Corp. (El Segundo, Calif.), Mar. 1967.

15. Kallet, Eli A.: Radiation Balance Horizon Sensors. Proceedings of the First Symposium on Infrared Sensors for Spacecraft Guidance and Control, Barnes Engineering Co. (Stamford, Conn.), May 1965.

16. Hagen, W. B.; and Nelson, J. L.: Final Report for Design, Development, Fabrication, and Evaluation Test of Reliable Earth Sensor. TRW no. 4106-6002-R0000. NAS 5-3408, Dec. 30, 1965.

17. Hieatt, James L.; and Hagen, William B.: Reliable Earth Sensor. Proceedings of the First Symposium on Infrared Sensors for Spacecraft Guidance and Control, Barnes Engineering Co. (Stamford, Conn.), May 1965.

18. DeWaard, Russell: High Irradiance on Thermistor Bolometers. Barnes Engineering Co. Engineering Memorandum, Nov. 29, 1966.

19. Weiner, Seymour: Infrared Detectors for Horizon Sensing Applications. Proceedings of the First Symposium on Infrared Sensors for Spacecraft Guidance and Control, Barnes Engineering Co. (Stamford, Conn.), May 1965.

20. Bates, Jerry C.; Hanson, David S.; House, Fred B.; Carpenter, Robert O'B.; and Gille, John C.: The Synthesis of 15 Micron Horizon Radiance Profiles from Meteorological Data Inputs. NASA CR-724, Apr. 1967.

21. Dodgen, J. A.; McKee, T. B.; and Jalink, A.: NASA-LRC Program to Define Experimentally the Earth's IR Horizon. Paper presented at the Second Symposium on Infrared Sensors for Spacecraft Guidance and Control, Aerospace Corp. (El Segundo, Calif.), Mar. 1967.

22. Vogelzang, W. F.; and Ohring, F.: The 15 Micron Infrared Horizon Radiance Profile; Temporal, Spatial, and Statistical Sampling Requirements for a Global Measurement Program. NASA CR-66190, Oct. 1966.

23. McKee, Thomas B.; Whitman, Ruth I.; and Davis, R. E.: Infrared Horizon Profiles for Summer Conditions From Project Scanner. NASA TN D-4741, Aug. 1968.

24. Whitman, Ruth I.; McKee, Thomas B.; and Davis, Richard E.: Infrared Horizon Profiles for Winter Conditions From Project Scanner, NASA TN D-4905, Dec. 1968.

25. Dodgen, John A.; and Curfman, Howard J., Jr.: Accuracy of IR Horizon Sensors as Affected by Atmospheric Considerations. A.F. rept. no. SAMSO TR-69-417, vol. I, Oct. 1969, pp. 161-167.

26. Wark, D. Q.; Alishouse, J.; and Yamamoto, G.: Calculations of the Earth's Spectral Radiance for Large Zenith Angles. Meteorological Satellite Laboratory Report no. 21, Oct. 1963.

27. Earle, M. D.: Infrared Horizon Sensor Accuracy in the Atmospheric Absorption Bands. ASTIA, AD-460971, Aerospace Corp., June 1964.

28. Thomas, John R.: Derivation and Statistical Comparison of Various Analytical Techniques which Define the Location of Reference Horizons in the Earth's Horizon Radiance Profile. NASA CR-726, Apr. 1967.

29. Ziolkowski, Adrian: Horizon Simulators for Sensor Testing. Proceedings of the First Symposium on Infrared Sensors for Spacecraft Guidance and Control, Barnes Engineering Co. (Stamford, Conn.), May 1965.

30. Burn, J. W.: Application of the Spectral and Spatial Characteristics of the Earth's Infrared Horizon to Horizon Scanners. IEEE Transactions on Aerospace Support Conference Procedures, vol. AS-1, no. 2, Aug. 1963.

31. Uplinger, W. G.; Burn, J. W.; Schmelzer, R. J.; and Morris, R. P.: The Earth's Limb for the 15 Micron Carbon Dioxide Absorption Band. Presented at the Second Symposium on Infrared Sensors for Spacecraft Guidance and Control, held at Aerospace Corp. (El Segundo, Calif.), Mar. 1967.

32. Nordberg, W.; McCulloch, A. W.; Foshee, L. L.; and Bandeen, W. R.: Preliminary Results From Nimbus II. NASA-TM-X-55638, Aug. 1966.

33. Johnson, Darrell W.: Horizon Definition Study Summary, Part I. NASA CR-66180, Oct. 1966.

34. Conrath, Barney J.: Earth Scan Analog Signal Relationships in the TIROS Radiation Experiment and their Application to the Problem of Horizon Sensing. NASA TN-D-1341.

35. Hanel, R. A.; Bandeen, W. R.; and Conrath, B. J.: The Infrared Horizon of the Planet Earth. NASA-GSFC Report no. X-650-62-164, Aug. 1962.

36. Wark, D. Q.; Alishouse, J.; and Yamamoto, G.: Variation of the Infrared Spectral Radiance Near the Limb of the Earth. Applied Optics, vol. 3, no. 3, Feb. 1964, pp. 221-227.

NASA SPACE VEHICLE DESIGN CRITERIA
MONOGRAPHS ISSUED TO DATE

SP-8001 (Structures)	Buffeting During Launch and Exit, May 1964
SP-8002 (Structures)	Flight-Loads Measurements During Launch and Exit, December 1964
SP-8003 (Structures)	Flutter, Buzz, and Divergence, July 1964
SP-8004 (Structures)	Panel Flutter, May 1965
SP-8005 (Environment)	Solar Electromagnetic Radiation, June 1965
SP-8006 (Structures)	Local Steady Aerodynamic Loads During Launch and Exit, May 1965
SP-8007 (Structures)	Buckling of Thin-Walled Circular Cylinders, revised August 1968
SP-8008 (Structures)	Prelaunch Ground Wind Loads, November 1965
SP-8009 (Structures)	Propellant Slosh Loads, August 1968
SP-8010 (Environment)	Models of Mars Atmosphere (1967), May 1968
SP-8011 (Environment)	Models of Venus Atmosphere (1968), December 1968
SP-8012 (Structures)	Natural Vibration Modal Analysis, September 1968
SP-8013 (Environment)	Meteoroid Environment Model–1969 (Near Earth to Lunar Surface), March 1969
SP-8014 (Structures)	Entry Thermal Protection, August 1968
SP-8015 (Guidance and Control)	Guidance and Navigation for Entry Vehicles, November 1968
SP-8016 (Guidance and Control)	Effects of Structural Flexibility on Spacecraft Control Systems, April 1969

SP-8017 (Environment)	Magnetic Fields–Earth and Extraterrestrial, March 1969
SP-8018 (Guidance and Control)	Spacecraft Magnetic Torques, March 1969
SP-8019 (Structures)	Buckling of Thin-Walled Truncated Cones, September 1968
SP-8020 (Environment)	Mars Surface Models (1969), May 1969
SP-8021 (Environment)	Models of Earth's Atmosphere (120 to 1000 km), May 1969
SP-8023 (Environment)	Lunar Surface Models, May 1969
SP-8024 (Guidance and Control)	Spacecraft Gravitational Torques, May 1969
SP-8025 (Chemical Propulsion)	Solid Rocket Motor Metal Cases, April 1970
SP-8027 (Guidance and Control)	Spacecraft Radiation Torques, October 1969
SP-8028 (Guidance and Control)	Entry Vehicle Control, November 1969
SP-8029 (Structures)	Aerodynamic and Rocket-Exhaust Heating During Launch and Ascent, May 1969
SP-8031 (Structures)	Slosh Suppression, May 1969
SP-8032 (Structures)	Buckling of Thin-Walled Doubly Curved Shells, August 1969
SP-8034 (Guidance and Control)	Spacecraft Mass Expulsion Torques, December 1969
SP-8035 (Structures)	Wind Loads During Ascent, June 1970

NASA-Langley, 1970 —— 14